



OPEN Study on mining-induced stress behavior on surrounding rock of rockburst mine under large buried depth and hard overburden

Xingen Ma^{1,3}, Bing Hu³, Eryu Wang^{2,4,6}✉, Qiangdi Geng², Zhiwen Liu⁵, Yongyuan Li³, Fulong Sun³, Bingshan Wang³ & Wei Wang³

Xinzhuang Coal Mine in Huaneng Qingyang Mining Area has geological characteristics such as large buried depth, thick topsoil and hard overburden, which is a typical kilometer-deep rockburst mine. Currently, the mine remains in the fundamental construction phase. This provides a theoretical foundation for the mine's subsequent production processes. , this paper studies the stress distribution law of surrounding rock in the stope of Xinzhuang Coal Mine. First of all, select the Panel 1 west wing of Coal 8 as a typical representative, and establish a large three-dimensional refined numerical model. Then, through numerical simulation research, the characteristics of surrounding rock abutment stress distribution zone in the mining process of the working face under complex conditions are obtained, which provides support for the regional design of rockburst prevention and control. The main research conclusions are as follows: (1) The research reveals the distribution characteristics of mining stress, elastic energy accumulation, and plastic zone at different widths of the first mining face, and determines the reasonable width of the working face. It is considered that the width of the working face can be greater than 175 m and less than 250 m, and the design width 200 m of the working face of Xinzhuang Coal Mine is reasonable. (2) The research reveals the evolution law and influence factors of mining stress, elastic energy accumulation and plastic zone distribution in the first mining face. The research results can not only provide theoretical support for the subsequent production of Xinzhuang Coal Mine, but also provide reference for the rockburst prevention and control work of mines with similar geological conditions.

Keywords Large buried depth, Thick topsoil, Hard overburden, Rockburst mine, Mining-induced stress behavior

The safe and efficient mining of coal resources is the eternal theme of the entire coal industry¹. With the depletion of shallow resources, China's mining depth extends to the deep at the rate of 10–15 m per year. According to statistics, 72% of mines buried more than 800 m face the threat of rockburst. Under the condition of thick topsoil and hard overburden, the stress field of surrounding rock shows strong nonlinear characteristics after mining disturbance, and the traditional theory is difficult to accurately predict the mechanism of rockburst. In the mining process of mining coal mine, mining activities will inevitably lead to the overburden movement and the redistribution of surrounding rock stress, so the prevention and control of mine pressure disasters is particularly important². Among all kinds of mine pressure disasters, rock burst disasters are extremely prompt and destructive, and have different mechanisms under different geological conditions, so it is very difficult to efficiently and accurately monitor, warn and prevent³.

In recent years, many scholars have conducted in-depth studies on the mechanical mechanism of rock burst generation, providing important references for the early warning and prevention of such disasters^{4,5}. Typical research achievements are as follows: Professor Dou Linming proposed the mechanism of dynamic and static load superimposed to induce scouring, and explained the interrelationship between high static load

¹China University of Mining and Technology, Xuzhou 221000, China. ²School of Mining and Coal Engineering, Inner Mongolia University of Science and Technology, Baotou 014010, China. ³Huaneng Coal Technology Research Co., Ltd., Beijing 100070, China. ⁴Inner Mongolia Yitai Group Co., Ltd., Ordos 017000, China. ⁵Huaneng Qingyang Coal Power Co., Ltd, Qingyang 745000, China. ⁶School of Mechanics and Civil Engineering, China University of Mining and Technology (Beijing), Beijing 100083, China. ✉email: 2019958@imust.edu.cn

condition of stope surrounding rock, dynamic load generation caused by overburden migration, and rockburst disaster⁶. Researcher Pan Junfeng conducted an in-depth study on the scour prevention mechanism of artificial liberated layer, and demonstrated the feasibility and effectiveness of active regional scour prevention measures⁷. Professor Wang Hongwei studied the abrupt effect of coupling instability of fault overlying rock and identified the mechanical relationship between fault slip instability and rock burst⁸. Professor Song Dazhao studied the mechanism of impact in near-upright coal seam mining, and proposed a static dynamic evaluation method for near-upright coal seam impact hazard.

Huaneng Qingyang Mining area is currently planned to have two pairs of mines, Walnut Yu coal mine and Xinzhuang Coal mine, both of which are kilometers deep and have typical geological characteristics such as thick topsoil and hard overlying rock. Walnut Yu coal mine has been put into operation in October 2020, during the mining period, the mine earthquake appeared obviously, and there were many large energy vibration events. Xinzhuang Coal Mine, which is adjacent to Walnut Yu Coal Mine, is expected to face more serious threat of rock burst disaster after putting into operation. In view of the fact that Xinzhuang Coal mine has not yet carried out relevant research on the mechanism of rock burst disaster, in order to provide a theoretical basis for the subsequent coal mine operation, this paper studies the stress behavior law of the surrounding rock of Xinzhuang Coal mine⁹.

Mine engineering overview

General situation of Qingyang mining area

Qingyang mining area has two coal mines, Walnut Yu Coal mine and Xinzhuang Coal mine, with large geological reserves, high coal quality and good market prospects. It is an important support for Longdong energy base and occupies an important position in the coal industry of Huaneng Group Company. However, the coal seams of the two mines are generally buried deep, and there are multiple disasters of Luohe Formation roof water damage, rock burst (mine earthquake), oil-type gas, coal seam spontaneous ignition and other disasters, which are mutually induced, so it is extremely difficult to govern the disaster. Binchang Mining area adjacent to similar conditions has now been defined by the State Administration of Mine Safety as “one of the mining areas with the heaviest coal disaster, the most difficult to govern, the highest safety risk, and the most heavy task of effectively preventing and containing major and major accidents”^{10,11}.

Qingyang Mining area has complex geological conditions such as large buried depth of coal seam, high stress of raw rock, complex hydrological conditions and the occurrence of thick hard roof. Its two coal mines are rock burst mines, among which the Huoyu coal mine started construction in 2009 and put into trial production in 2020, and the Xinzhuang Coal mine started construction in 2013. At present, it is still in the construction period, and it is planned to start production in 2024. The mine earthquake phenomena occurred in both mines during the period of roadway excavation and initial operation. In view of the above situation, Qingyang mining area has planned a number of rock burst research projects in recent years, and carried out a certain amount of research work, but the overall research foundation is still relatively weak.

Overview of Xinzhuang coal mine

Xinzhuang Coal Mine is located about 15 km south of Ningxian County, Qingyang City, Gansu Province, the administrative division of Xinzhuang Town and Zhongcun Township, Ningxian County, geographical coordinates: 107°43′59″–107°59′55″ east longitude; North latitude 35°14′41″–35°22′19″, east–west length of about 20.0 km, north–south width of 7.6–12.5 km, an area of 206.2823 km², the design capacity of 8Mt/a.

The Xinzhuang minefield contains coal layers 5–1, 5–2 and 8, which are three recoverable coal layers (see Table 1). Among them, the coal 5–1 layer and the coal 5–2 layer belong to relatively stable and mineable coal seam, which is the minor mineable coal seam in the minefield. The 8 layer of coal belongs to relatively stable and recoverable coal seam, which is the main recoverable coal seam in the minefield. The spacing between coal layer 5–1 and coal layer 5–2 is 0.81–15.13 m, and the spacing between coal layer 5–2 and coal layer 8 is 1.66–58.41 m.

Coal layer 8 is the coal seam of the main mining seam and the coal seam to which the first mining face belongs and the coal seam and the bottom floor have weak impact tendency. The roof of coal seam is mainly mudstone, followed by silty mudstone or argillaceous siltstone, and occasionally siltstone and coarse sandstone roof. The coal seam floor is dominated by siltstone, sandy mudstone and carbonaceous mudstone, and partially by mudstone and argillaceous siltstone, and occasionally coarse sandstone floor. The coal layer 8 is to adopt the full-mechanized mining method of caving top coal. The design mining height is 3.5 m, the width of working face is 200–250 m, and the advancing length is 2500–5000 m.

Coal seam number	Minable coal seam Minimum to maximum average	Coal seam structure	Gangue layer	Gangue thickness	Mining index	Minability	Stability
Coal 5–1	0.85–3.48 2.25	Simple	0–1	0.1–0.78	71	Mostly mineable	Relatively stable
Coal 5–2	0.85–4.49 1.28	Simple	0–2	0.1–0.6	72	Mostly mineable	Relatively stable
Coal 8	0.88–4.49 8.71	Simple	0–2	0.1–2.1	95	Mostly mineable	Relatively stable

Table 1. List of characteristics of coal seams that can be mined.

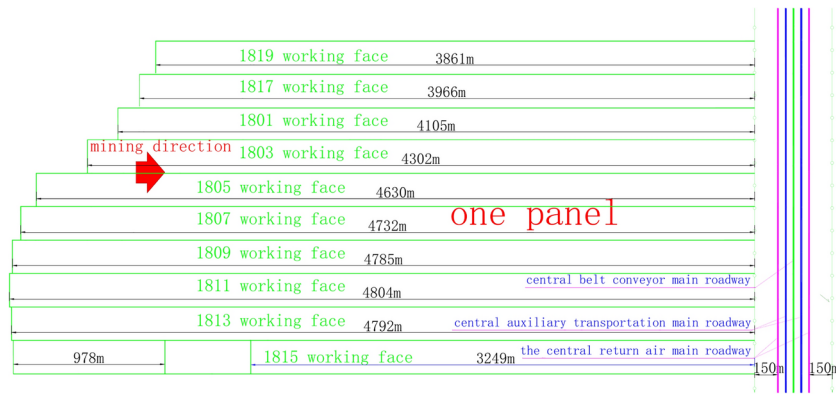


Fig. 1. Modeling scope of the numerical model.

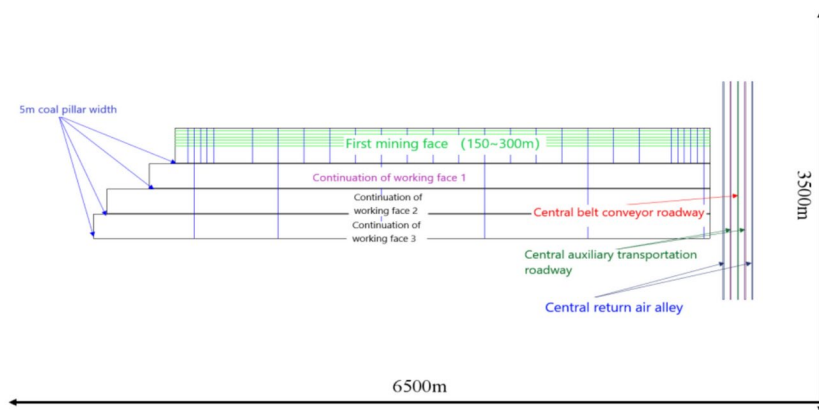


Fig. 2. Working face layout of the west wing of the first pan area of coal mine.

Numerical model establishment and simulation scheme

The first mining area of Xinzhuang Coal mine is a pan area, and the main recoverable coal seam is 8 layers of coal. Therefore, this simulation takes the mining of coal face in the 8-pan area as the main research object, in order to obtain the abutment stress, elastic energy and plastic zone distribution characteristics of surrounding rock during the mining process under complex conditions such as large buried depth, thick topsoil and hard overlying rock, and provide support for regional anti-impact design.

Modeling scope

According to the supplementary exploration data of the previous mining area, the coal seams in Coal 8 Plate 1 area are relatively stable, and the thickness of the coal seams is gradually thinning at the southern stripping boundary. Not affected by the stubble of the overlying coal seam, in order to put the mine into production as soon as possible and reach production, the design of the first mining face of Coal 8 Plate Area is arranged in the western part of the plate area, and according to the mining and digging succession plan of Coal 8 Plate Area, the mining range of the working face of the western wing of Coal 8 Plate Area is selected as the main modeling area.

Geodetic coordinates X coordinate range: 36484904.4203–36491404.4203 m, Y coordinate range: 3906759.8339–3910259.8339 m, and Z coordinate range: – 400 m to the surface of the ground, to carry out the large-size three-dimensional refinement modeling, the model size of 6500 m × 3500 m × 1680 m, the modeling area is shown in Fig. 1.

The complex conditions such as the change of surface soil thickness, the change of buried depth of coal seam, the change of coal seam thickness, the change of coal seam inclination, the change of hard roof thickness, and the syncline structure are included in the established numerical model, which is typical of Xinzhuang Coal mine.

Construction of numerical model

According to the connection plan of the stoping face in Coal8 No.1 block of Xinzhuang Coal Mine, the layout of the working face in the west wing of Coal8 No.1 block of Xinzhuang Coal Mine and the layout of the central return air main roadway, the central auxiliary transportation main roadway and the central belt conveyor main roadway, the layout of the working face in Coal8 No.1 block is shown in Fig. 2. The width of the first mining face is preset to be 150–300 m (the design width of the mine is 200 m), and the width of the coal pillar in the section between the first mining face and the adjacent successive working face 1 is preset to be 5 m, and the width of the

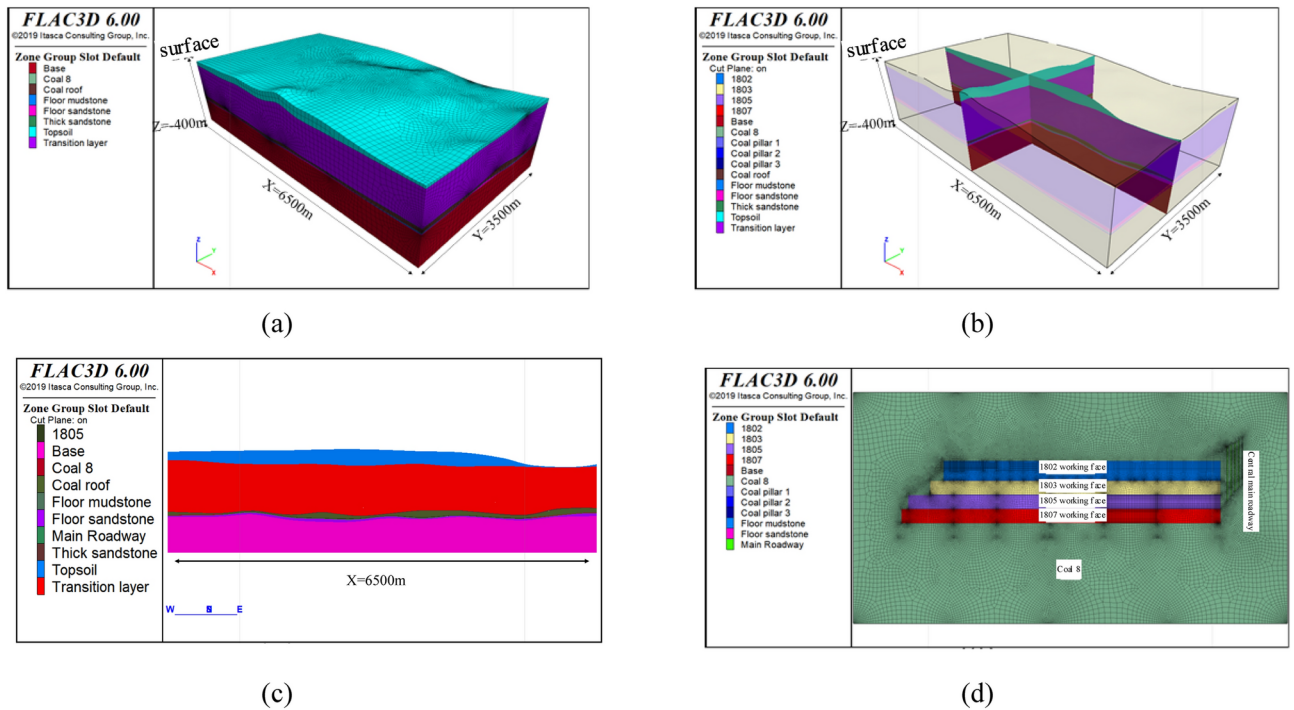


Fig. 3. 3D numerical model: (a) Three-dimensional numerical model; (b) Model internal slicing; (c) Model to slice ($Y = 1750 \text{ m}$); (d) Layout of the working face in the model. (Generated by the software FLAC3D 6.00. URL link: <https://www.itascacg.com/software/FLAC3D>).

Stratum	maxDensity (Kg/m ³)	seamModulus of elasticity (GPa)	Poisson's ratio	Cohesion (MPa)	Angle of internal friction (°)	Minability tensile strength (MPa)
Loess	1640	0.185	0.14	0.0938	34.5	0.35
Transition layer	2541	8.136	0.25	4.8	34.21	2.81
Thick sandstone	2618	11.62	0.22	4.249	34.00	3.17
Coal roof	2548	6.48	0.17	2.505	25.97	2.7
Coal 8	1390	2.607	0.25	2	24.80	1.97
Mudstone floor	2200	3.07	0.25	2.37	26.21	1.91
Sandstone floor	2447	9.28	0.26	4.408	34.05	1.78
bedrock	2550	14	0.24	5.62	33.31	2.81

Table 2. Table of physical and mechanical parameters of coal and rock mass for numerical simulation.

coal pillar between the successive working face 2 and 3 is preset to be 5 m. The distance between the stop-mining line of each working face and the nearest central return air main lane is 150 m, the section size of the central main lane is 6 m × 6 m, and the interval between the main lanes is 50 m.

The 3D numerical simulation was established based on the borehole exploration information and the continuous layout of the working face. The model is 6500 m long and 3500 m long. The bottom elevation of the model is - 400 m, the top elevation of the model is + 1280 m and the minimum is + 880 m. There are 2,315,212 units with 1,021,362 nodes. In the model, 1802 face ($X = 1350\text{--}5450 \text{ m}$, $Y = 2165\text{--}2465 \text{ m}$), 1803 face, 1805 face and 1807 face are preset, and 5 m wide coal pillars are set between each adjacent face. Five central alleys are arranged on the east side of the preset stoping line of each face. From west to east are the central return air main lane, the central auxiliary transport main lane, the central belt conveyor main lane. The 3D numerical model is shown in Fig. 3.

According to the ground stress conditions, normal displacement is fixed on both sides of the model in X and Y directions and horizontal stress is applied. Fixed normal displacement at the bottom of the model; The top of the model is the surface, and the free boundary is set. G is set to 10 m/s². The Moore-Coulomb criterion model is adopted for numerical calculation. The physical and mechanical parameters of coal and rock mass in this study are shown in Table 2^{12,13}.

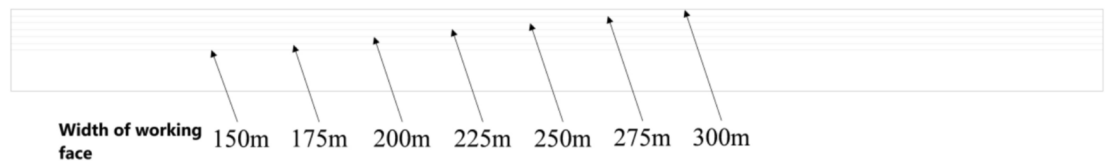


Fig. 4. Schematic diagram of simulation study on different widths of first mining face.

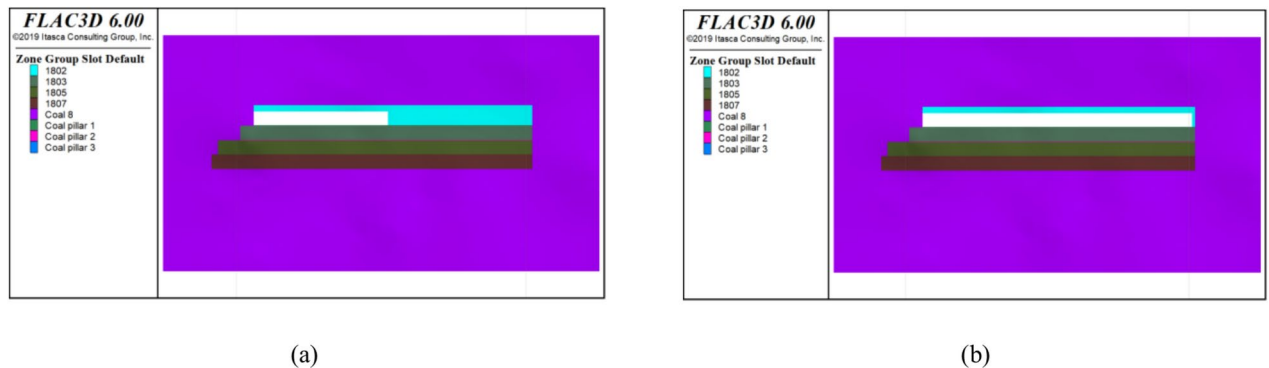


Fig. 5. Schematic diagram of step-by-step excavation for study of working face width: (a) 2000 m excavation of 1802 face; (b) Excavation of the 1802 face for another 2100 m.

Numerical simulation scheme

Excavation scheme for numerical simulation of working face width

Face width plays a critical role in the mining process. The maximum height of the formation separation rupture is closely correlated with the size of the gob, extending from the cutting hole to the full mining stage. Therefore, the width of the working face has an important influence on the appearance of rock burst disaster in the mine^{14–18}. In order to study the influence of different stoping widths on the adjacent working face to be worked, the distribution characteristics and peak position of lateral supporting stress, elastic strain energy and peak value of surrounding rock, and the distribution of impact risk of surrounding rock, this paper takes the 1802 working face of Coal Mine No. 8 in Yipan District of Xinzhuang Coal Mine as an example. When 1802 working face width is 150, 175, 200, 225, 250, 275, 300 m, the stress and energy field, plastic zone of surrounding rock are studied, as shown in Fig. 4.

The excavation scheme of the face width simulation study is as follows:

- (1) Based on the stress balance results of the original rock, the central return air main lane, central auxiliary transportation main lane and central belt conveyor main lane on the east side of the excavation model are calculated for balance;
- (2) Based on the balance calculation results after the excavation of the central main lane, the 1802 working face (4100 m long) is excavated in two times. The first excavation is 2000 m and the calculation is balanced; Then the 1802 working face was excavated 2100 m to calculate the balance. The excavation diagram of the working face is shown in Fig. 5.
- (3) The excavation scheme simulated by the “three fields” evolution law of surrounding rock during the mining process of the working face.
 - (1) Numerical simulation excavation scheme of the “square” process of the first mining face

In order to analyze and study the distribution and evolution characteristics of stress and elastic strain energy of surrounding rock at the boundary of the 1802 face, the distribution law of rock burst risk of surrounding rock before and after “square” of the 1802 face is studied. Taking the first mining face of 1802 as the research object, the 1802 working face is excavated to 100, 150, 200 (square), 250 and 300 m in turn with the excavation step of 50 m. After each excavation, the balance is solved, and then the excavation is carried out according to the 400 m step, as shown in Figs. 6 and 7.

- (2) Numerical simulation excavation scheme for the mining process of the first mining face

In order to study the distribution and evolution characteristics of supporting stress, peak stress, elastic strain energy and peak elastic strain energy of surrounding rock during the mining process of working face, analyze the influence of complex geological conditions such as surface elevation, yellow soil thickness, coal seam depth, hard roof strata, coal seam thickness and dip Angle changes, and delineate the concentrated areas of high stress and high elastic energy. It provides theoretical basis for rock burst prevention and control in actual mining of



Fig. 6. Schematic diagram of simulation study of first mining working face advance process.

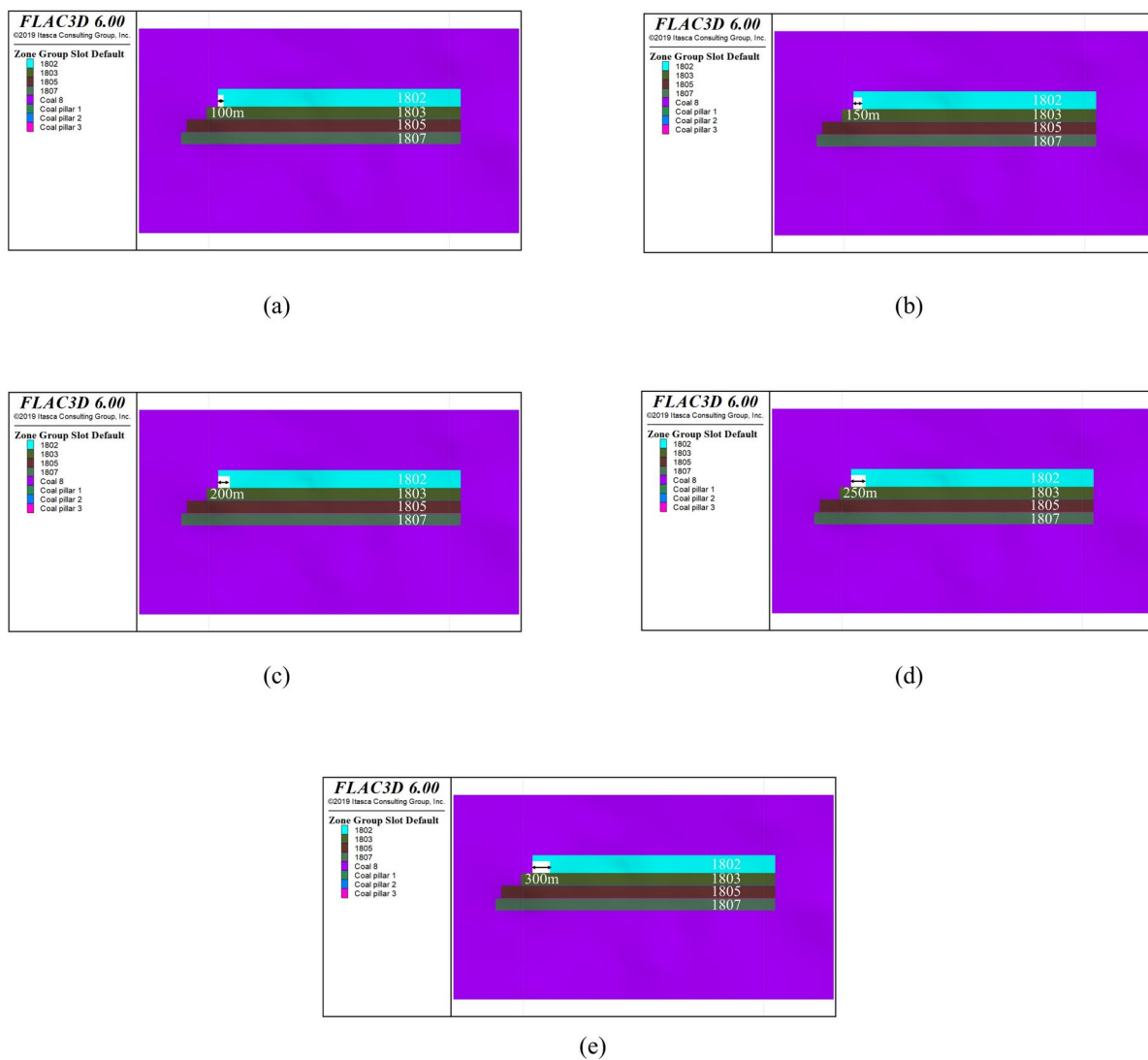


Fig. 7. Schematic diagram of “square” excavation of 1802 working face: (a) Excavate 100 m; (b) Excavate 150 m; (c) Excavate 200 m; (d) Excavate 250 m; (e) Excavate 300 m.

working face. The following excavation scheme is designed. After the 1802 face is “squared”, the overall stopping face 1802 with a excavation step of 400 m is adopted, and the equilibrium is solved after each excavation, as shown in Fig. 8.

The numerical simulation analysis Study of reasonable width of working face

Distribution and evolutionary characteristics of “multi-field” of surrounding rocks with different working face widths

(1) Evolutionary law of mining stress distribution

According to the excavation steps shown in Fig. 9, seven cases were simulated when the width of 1802 first mining face was 150, 175, 200, 225, 250, 275 and 300 m. The stress distribution of the surrounding rock of the working face under the seven different widths of the 1802 first mining face was extracted respectively, as shown in Fig. 9.

From the Fig. 9, it can be seen that as the width of the 1802 working face increases from 150 to 300 m, the surrounding rock stress increases as a whole, and the peak stresses of the coal seam are 54.15, 62.31, 62.87, 62.49, 63.32, 67.76, 76.99 MPa in the following order, the peak stresses of the surrounding rock in the X = 3230 m section are 49.44, 52.26, 54.88, 57.28, 59.48, 61.53 and 63.37 MPa. Overall, the surrounding rock stress gradually increased with the increase of the width of the working face, but the distribution characteristics of the surrounding rock stress in the working face did not change significantly.

(2) Distribution and evolutionary law of plastic zone

The distribution status of the plastic zone in the working face under 7 different widths of 1802 first mining face was extracted respectively, as shown in Fig. 10. It can be seen from the plane distribution map of plastic zone, 1802 working face boundary plastic area is mainly distributed in the range of 5–20 m from the goaf boundary, the plastic zone near the first cutting of the working face and the stopping line in the direction of the strike is smaller, and the plastic zone in the central mining boundary of the working face is larger, and comparing the distribution of the plastic zone of the working face surrounding rock under different width conditions, it can be seen that, with the increase of the width, the distribution characteristics of the plastic zone in the direction of the working face have not changed significantly.

According to the distribution of plastic zone profile in Fig. 10, it can be seen that the roof and floor of the goaf are affected by the mining activities and plastic failure occurs to a certain extent. The plastic failure area of the floor under the goaf is within 15–20 m from the goaf boundary, mainly distributed in the mudstone bottom plate and thin sandstone bottom plate under the goaf. The depth of the plastic zone under the goaf changes with the thickness of the mudstone and thin sandstone bottom plate, and the thicker the bottom plate, the deeper the plastic zone extends downward. The plastic zone of the surrounding rock above the goaf is also mainly concentrated in the complex rock formation with the thickness of a single layer less than 10 m above Coal 8 and the thick sandstone with the thickness of the first layer above Coal 8 exceeding 10 m. Plastic failure areas in the rock layers above the thick sandstone are sparsely distributed, and plastic failure rock masses that develop towards the interior of the goaf only appear above the boundaries on both sides of the goaf. Comparative analysis of the distribution of the plastic zone above the 1802 goaf under different width conditions shows that with the increase of the width of the working face the plastic zone in the middle of the tendency of the goaf has not changed significantly, and the height of the plastic zone development is 20–30 m above the coal seam; However, the plastic zone above the two sides of the goaf gradually increases and develops towards the middle of the tendency of the goaf. When the width of the working face increases from 150 to 300 m, the development height of the plastic zone on both sides of the goaf increases from 34 m above the goaf to 93 m, and develops towards the middle of the goaf by about 41 m.

(3) Evolutionary law of elastic energy distribution

The elastic energy density distribution states of the working face at seven different widths of the 1802 first mining face were extracted separately, as shown in Fig. 11. It can be seen from the planar distribution diagram of elastic energy density of coal seam that the elastic energy of surrounding rock is mainly concentrated in the range of 20–200 m from the boundary of 1802 goaf, and the range of elastic energy concentration along the strike direction of the working face near the open-off cut and the stopping line is smaller, and the range of elastic energy concentration in the surrounding rock in the middle of the working face at the boundary of the goaf is larger. From the distribution diagram of elastic energy density profile, it can be seen that the elastic energy density is mainly concentrated in the coal8 and its roof and floor rock layer, and the elastic energy density of the surrounding rock of other rock layer groups is small, mainly because the elastic modulus of the coal mass is smaller than the elastic modulus of the rock mass. The peak elastic energy of coal is mainly concentrated at the goaf boundary on both sides of the working face, and the peak elastic energy is about 15–20 m away from the goaf boundary. With the increase of the width of the working face, the concentration of the elastic energy of the surrounding rock increases, but the characteristics of the distribution of the elastic energy have not changed significantly.

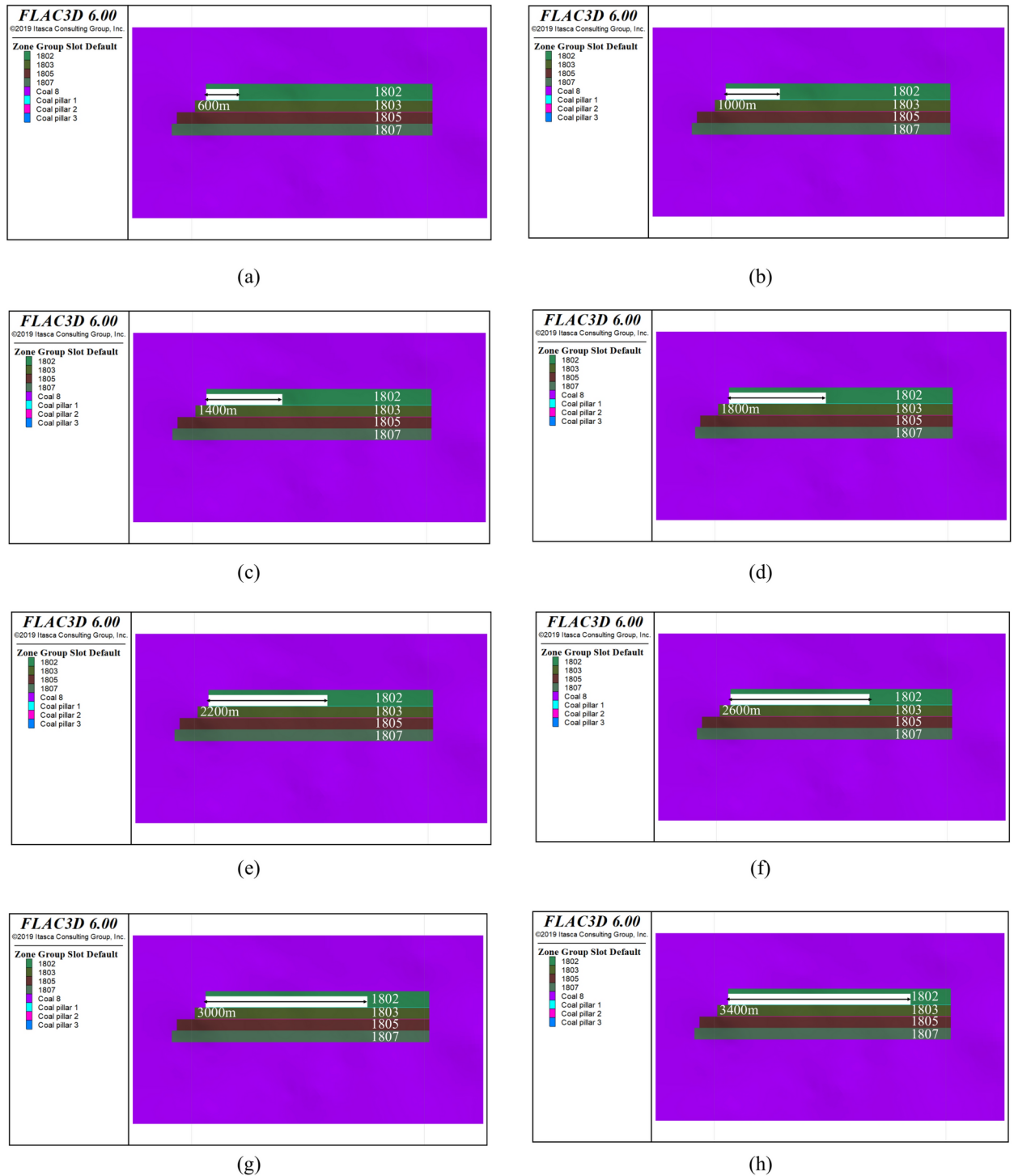


Fig. 8. Schematic diagram of mining process of 1802 working face: (a) Excavate 600 m; (b) Excavate 1000 m; (c) Excavate 1400 m; (d) Excavate 1800 m; (e) Excavate 2200 m; (f) Excavate 2600 m; (g) Excavate 3000 m; (h) Excavate 3400 m.

Determination of the reasonable width of the working face

In order to analyze the influence result of the working face width on the surrounding rock stress, the vertical stress curve distributed along the coal seam at the section where $X = 3230$ m is extracted, as shown in Fig. 12. At the position where $Y = 2165$ m, it is the south goaf boundary of the 1802 working face, and at the position where $Y = 2315\text{--}2465$ m, it is the north goaf boundary of the 1802 working face affected by geological factors such as the distance between the coal seam thickness and the hard roof, and the buried depth of the coal seam, as the width of the 1802 working face increases from 150 to 300 m, the surrounding rock stress concentration area and the stress peak position continue to migrate and evolve. Therefore, there is no obvious rule for the stress

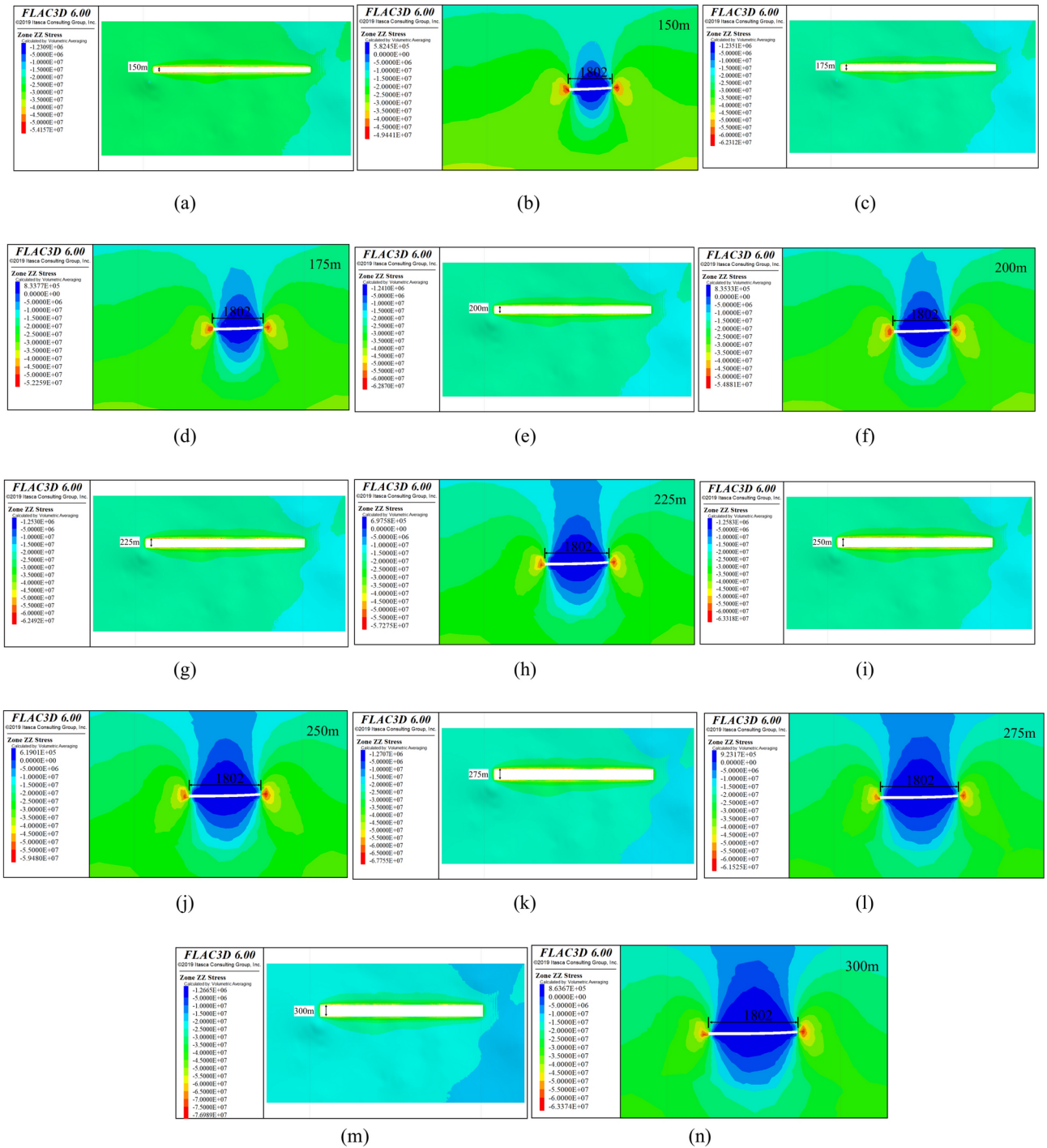


Fig. 9. Stress distribution in the surrounding rock of the working face under different width conditions (The profile is X=3230m): (a) Plane stress diagram of working face with a width of 150m; (b) Profile stress diagram of working face with a width of 150m; (c) Plane stress diagram of working face with a width of 175m; (d) Profile stress diagram of working face with a width of 175m; (e) Plane stress diagram of working face with a width of 200m; (f) Profile stress diagram of working face with a width of 200m; (g) Plane stress diagram of working face with a width of 225m; (h) Profile stress diagram of working face with a width of 225m; (i) Plane stress diagram of working face with a width of 250m; (j) Profile stress diagram of working face with a width of 250m; (k) Plane stress diagram of working face with a width of 275m; (l) Profile stress diagram of working face with a width of 275m; (m) Plane stress diagram of working face with a width of 300m; (n) Profile stress diagram of working face with a width of 300m.

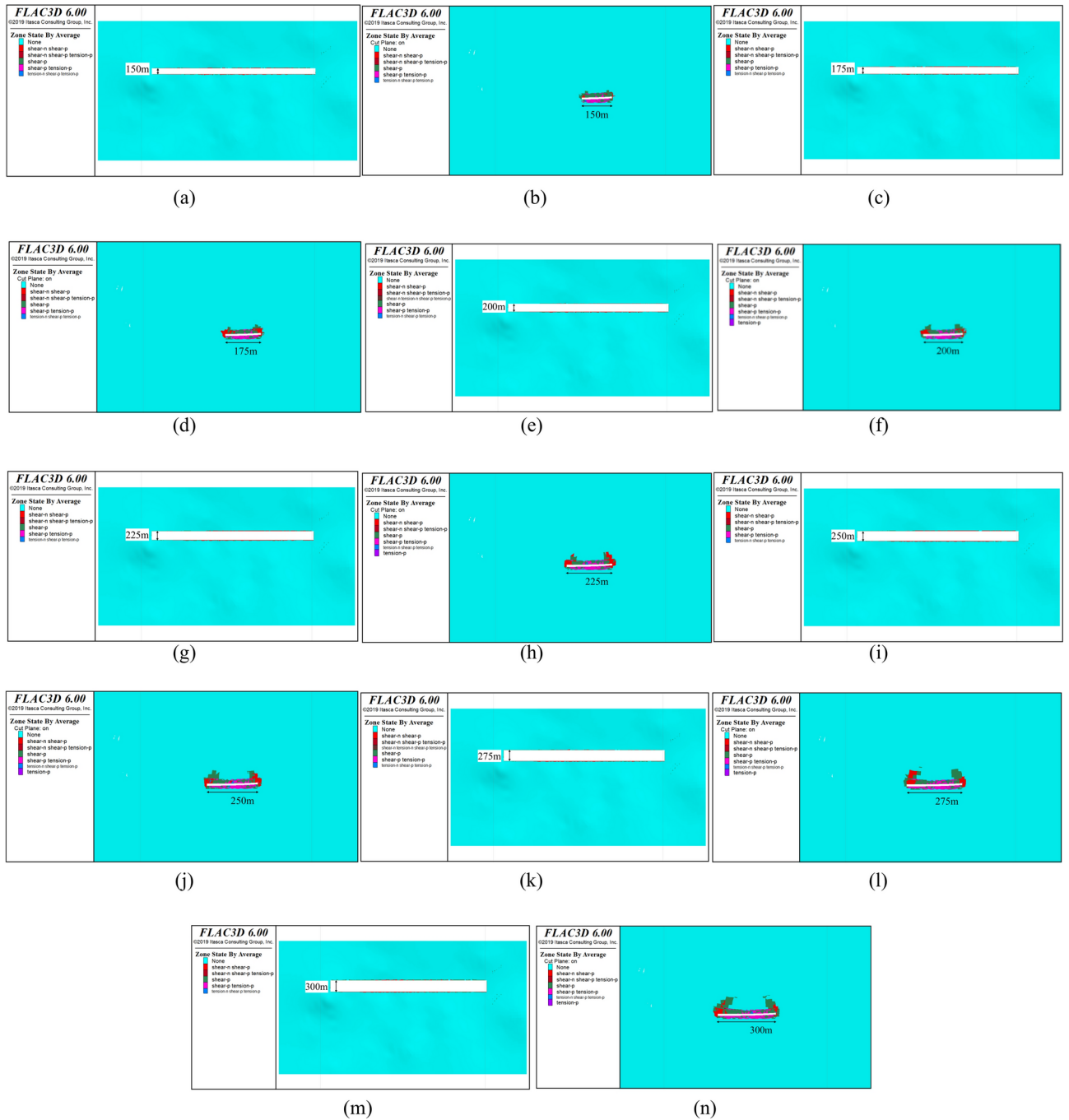


Fig. 10. Distribution of plastic zone in the surrounding rock of the working face under different width conditions (The profile is $X = 3230\text{ m}$): (a) Plane distribution of the plastic zone with a working face width of 150 m; (b) Profile distribution of plastic zone with a working face width of 150 m; (c) Plane distribution of the plastic zone with a working face width of 175 m; (d) Profile distribution of plastic zone with a working face width of 175 m; (e) Plane distribution of the plastic zone with a working face width of 200 m; (f) Profile distribution of plastic zone with a working face width of 200 m; (g) Plane distribution of the plastic zone with a working face width of 225 m; (h) Profile distribution of plastic zone with a working face width of 225 m; (i) Plane distribution of the plastic zone with a working face width of 250 m; (j) Profile distribution of plastic zone with a working face width of 250 m; (k) Plane distribution of the plastic zone with a working face width of 275 m; (l) Profile distribution of plastic zone with a working face width of 275 m; (m) Plane distribution of the plastic zone with a working face width of 300 m; (n) Profile distribution of plastic zone with a working face width of 300 m.

peak of the surrounding rock on the side of $Y = 2315\text{--}2465$ m, and the stress peak of the surrounding rock of the goaf boundary at $Y = 2165$ m increases from 43.43 to 55.75 MPa, indicating that the wider the width of the working face, the more intense the overlying roof rock stratum movement, and the greater the lateral bearing stress in the goaf.

Extract the evolution characteristics of the elastic strain energy distribution of the surrounding rock of the goaf boundary on the south side of the 1802 working face ($Y = 2165$ m, fixed boundary) at the horizontal position of section $X = 3230$ m and $Z = 115$ m, as shown in Fig. 13. From Fig. 13a, it can be known that the stress distribution of the surrounding rock at the +115 m level is basically consistent with the stress distribution characteristics along the coal seam, and the concentrated stress increases with the increase of the width of the working face. When the width of the working face increases from 150 to 300 m, the vertical stress peak values are 47.7, 50.4, 53.0, 55.3, 57.5, 59.6, 61.5 MPa respectively, and the stress peak value is about 20 m away from the goaf boundary. From Fig. 13b, it can be known that the elastic energy change of the surrounding rock of the 1802 goaf boundary is similar to the evolution characteristics of the vertical stress distribution. As it extends from the goaf boundary to the solid coal, the elastic energy of the surrounding rock increases rapidly, and it reaches the peak of elastic energy within the range of about 10–15 m away from the goaf boundary, with a peak value of about 400–640 kJ/m³. After that, the elastic energy of the surrounding rock rapidly decreases within the range of 20–30 m away from the goaf boundary. When the distance between the surrounding rock and the goaf boundary is greater than 30 m, the rate of reduction of the elastic strain energy slows down; when the distance between the surrounding rock and the goaf boundary is about 150 m, the increase in the elastic strain energy of the surrounding rock compared with before mining has decreased to a relatively small value, indicating that the influence of the 1802 goaf on the stress and elastic strain energy distribution of the coal and rock mass outside 150 m is relatively small. As the width of the working face increases from 150 to 300 m, the position of the peak elastic energy shifts from 10 m away from the goaf boundary to 15 m away from the goaf boundary. The peak elastic strain energy of the goaf boundary is 400, 444, 486, 526, 566, 604, 640 kJ/m³ respectively, and the wider the working face, the more concentrated the elastic energy of the surrounding rock.

Extract the distribution and evolution characteristics of the elastic strain energy of the surrounding rock at the goaf boundary on the north side (variation boundary) of the 1802 working face at the section of $X = 3230$ m and $Z = 107$ m, as shown in Fig. 14. From Fig. 14a, it can be known that as the width of the working face increases from 150 to 300 m, the stress of the surrounding rock at the $Z = 107$ m level as a whole shows an increasing trend, and the stress peaks are 46.5, 48.4, 48.8, 50.7, 51.7, 53.3, and 55.4 MPa in turn. From Fig. 14b, it can be known that affected by geological factors such as the buried depth of the coal seam, the elevation of the coal seam, and the distance from the thick and hard roof, the stress and elastic energy concentration area at the goaf boundary on the northside continuously migrates and evolves with the change of the width of the working face. As the width of the working face increases from 150 to 300 m, the elastic energy density of the surrounding rock at the $Z = 107$ m level does not show a clearly increasing or decreasing rule, and the elastic energy peaks are 420.3, 392.8, 372.6, 425.6, 419.9, 456.3, and 504.6 kJ/m³ in turn. By comparing the distribution of surrounding rock stress and elastic energy at the goaf boundaries on both sides of the 1802 working face (Figs. 13 and 14), it can be known that the distance between the coal seam and the thick sandstone at the goaf boundary on the southside of the working face is generally smaller than that on the northside of the working face, and the concentration degree of surrounding rock stress and elastic energy at the goaf boundary on the south side ($Y = 2165$ m) of the working face is generally higher than that on the north side ($Y = 2315\text{--}2465$ m).

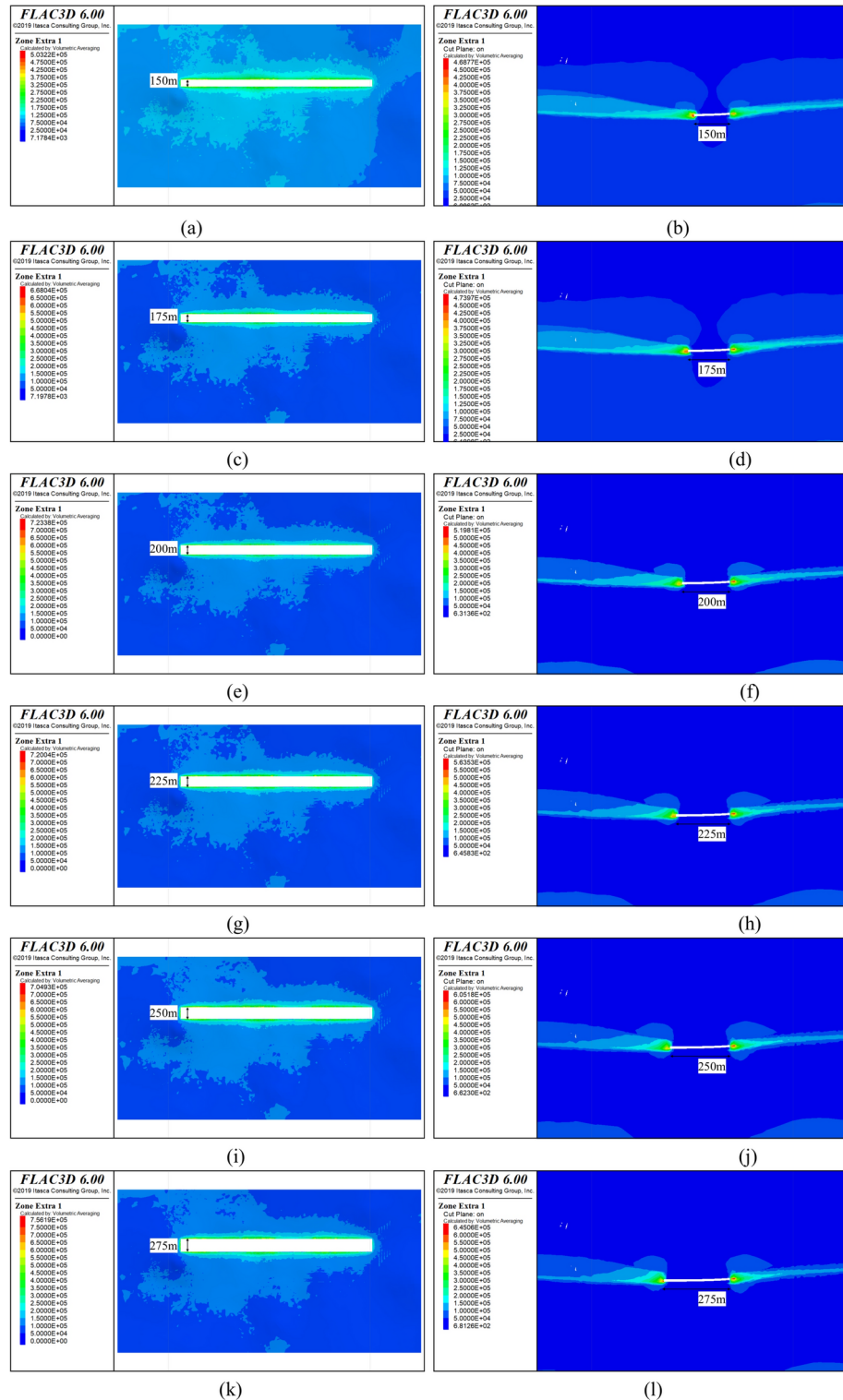
In a word, as the width of the working face increases, the concentration degree of the surrounding rock stress and elastic energy also goes up. The stress peak is about 15–20 m away from the goaf boundary, and the elastic energy peak is about 20 m away from the goaf boundary. The lateral bearing stress influence range of the 1802 working face is approximately 200–250 m.

Based on the impact of the working face width on the impact hazard in the impact ground pressure risk index evaluation form affected by mining technical factors, when the working face width is less than 100 m, the impact hazard evaluation index is 3 (the highest); when the working face width is 100–150 m, the impact hazard evaluation index is 2; when the working face width is 150–300 m, the impact hazard evaluation index is 1; when the working face width is greater than 300 m, the impact hazard evaluation index is 0. The higher the evaluation index, the higher the impact hazard. Therefore, when arranging the working face, it is necessary to avoid the working face width causing a higher impact hazard evaluation index. From this perspective, the working face width should be as large as possible.

On the other hand, when considering the stress concentration factor of the surrounding rock and the development height of the plastic zone, it can be observed that an increase in the working face width corresponds to a higher peak stress in the coal seam and a greater development height of the plastic zone. This indicates that the movement of the overlying rock above the coal seam becomes more pronounced, thereby intensifying the degree of mining disturbance. From Fig. 15, it can be known that the peak stress of the dip section of the working face approximately increases linearly with the increase of the working face width; the peak stress in the coal seam shows 3 step-like increases with the increase of the working face width, which are located at the working face width of 175, 275, and 300 m respectively, and the difference in the peak stress of the coal seam when the working face width is 175–250 m is relatively small; at the same time, the developing height of the plastic zone above the coal seam increases significantly with the increase of the working face width at 225–250 m; through comprehensive analysis, it is considered that the reasonable width of the working face can be taken as greater than 175 m and less than 250 m.

The evolution law of “multiple fields” in the mining of first working face

Based on the mine working face connection plan and the layout of the first mining working face 1802, under the condition that the width of the first mining working face is 200 m, based on the three-dimensional numerical



model of the panel, the evolution laws of the surrounding rock stress field, energy field, etc. during the recovery process of the 1802 working face are simulated and studied.

The stress distribution characteristics of the surrounding rock during the “squaring” process of the first mining face
 Based on the design of the 1802 working face, the working face “squared” when it was excavated to 200 m. The 1802 working face was excavated sequentially to 100, 150, 200, 250, and 300 m to study the evolution characteristics of the stress distribution of the surrounding rock before and after the working face “squared”. The stress distribution at the goaf boundary is shown in Fig. 16. From Fig. 16, it can be known that during the “squaring” process of the 1802 working face, as the length of the working face excavation increases from 100 to 300 m, the degree of stress concentration at the goaf boundary and the range of the peak zone gradually increase. By studying the evolution law of the stress distribution of the surrounding rock on the four sides of the working

◀ **Fig. 11.** Distribution of elastic energy of the surrounding rock in the working face under different width conditions (The profile is $X = 3230$ m): (a) Plane distribution of elastic energy with a working face width of 150 m; (b) Profile distribution of elastic energy for a working face width of 150 m; (c) Plane distribution of elastic energy for a working face width of 175 m; (d) Profile distribution of elastic energy with a working face width of 175 m; (e) Plane distribution of elastic energy with a working face width of 200 m; (f) Profile distribution of elastic energy with a working face width of 200 m; (g) Plane distribution of elastic energy with a working face width of 225 m; (h) Profile distribution of elastic energy with a working face width of 225 m; (i) Plane distribution of elastic energy with a working face width of 250 m; (j) Profile distribution of elastic energy with a working face width of 250 m; (k) Plane distribution of elastic energy with a working face width of 275 m; (l) Profile distribution of elastic energy with a working face width of 275 m; (m) Plane distribution of elastic energy with a working face width of 300 m; (n) Profile distribution of elastic energy with a working face width of 300 m.

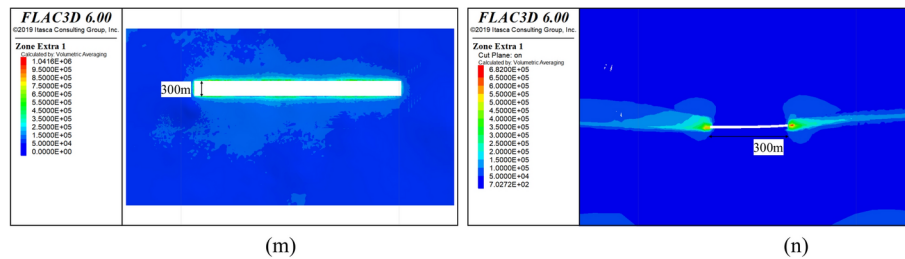


Figure 11. (continued)

face boundary, it can be known that as the recovery length increases, the stress peak and the high-stress zone gradually shift from the goaf boundaries on the east and west sides to the goaf boundaries on the north and south sides, that is, from the advanced coal wall of the working face to the lateral coal body.

In order to further analyze the evolution and transition process of the stress of the surrounding rock on the four sides of the goaf boundary and the stress peak zone, the stress distribution curves of the goaf boundary on the side of the working face open-off cut and the southside are extracted, as shown in Fig. 17. By comparing the evolution characteristics of the stress distribution of the surrounding rock on the side of the open-off cut and the southside boundary of the goaf, it can be known before the working face “squared”, as the excavation length increases from 100 to 200 m, the stress peak of the surrounding rock on the side of the open-off cut is 36.5, 39.0, and 40 MPa in turn, and the stress peak of the south side goaf boundary is 29.7, 34.4, and 38.8 MPa in turn. At this time, the excavation length is less than the width of the working face, the side of the open-off cut is the long side of the goaf, and the southside is the short side, so the degree of stress concentration of the surrounding rock on the side of the open-off cut and the mining field boundary is greater than that on the north and south sides of the goaf boundary.

When the length of the working face excavation is 250 and 300 m, and the length of the excavation is greater than the width of the working face, the stress peak of the surrounding rock on the side boundary of the open-off cut is 40.6 and 41.0 MPa in turn, and the stress peak of the surrounding rock on the south side of the goaf is 42.4 and 45 MPa in turn. The side of the open-off cut is the short side of the goaf, and the southside is the long side. The surrounding rock stress and peak value shift from the side of the open-off cut to the north and southside boundaries. From Fig. 17a and b, it can be known that with the increase of the excavation length, the distribution characteristics of the surrounding rock stress on the side of the open-off cut and the position of the stress peak do not change, but the stress gradually increases and the increase rate gradually decreases, indicating that the movement of the overlying rock on the side of the open-off cut tends to be stable; the stress peak of the surrounding rock on the goaf boundaries on the north and south sides of the working face maintains a large growth, and the position of the stress peak zone gradually shifts with the increase of the mining length, and the whole is located in the middle of the goaf boundary.

The distribution and evolution characteristics of the “multiple fields” in the mining process of the first working face

(1) The evolution law of the distribution of mining-induced stress

The tendency width of the 1802 working face is 200 m, and the strike length is as long as 4100 m. The strike direction span of the working face is large, and the ground layers fluctuate and change, and the geological conditions are relatively complex. Therefore, it is necessary to study the distribution and evolution characteristics of the surrounding rock stress, elastic energy, and plastic zone during the mining process of the 1802 working face. Figure 18 is the plane distribution and profile distribution diagram of the surrounding rock stress during the mining process of the working face.

Analyzing Fig. 18, it can be known that affected by the distribution of stress in the panel area, during the mining process of the 1802 working face, the overall peak value of the advanced bearing stress of the working face (not higher than 45 MPa) is smaller than the peak value of the lateral bearing stress of the working face. It can be seen from the figure that the elevation of Coal 8 at the section of $Y = 2265$ m, the buried depth of the

working face, and the ground elevation, etc. continuously change along the strike of the 1802 working face. When the working face is mined from 600 to 3900 m, the peak values of the section stress are 42.82, 43.61, 43.60, 43.59, and 43.59 MPa in turn, indicating that although the length of the working face mining is constantly increasing, under the influence of geological factors such as the buried depth of the coal seam, the distance between it and the thick and hard roof, and the thickness of the loesslayer, the peak value of the bearing stress in front of the stope undergoes a certain degree of fluctuation but the change is not obvious.

(2) The evolution law of the distribution of elastic energy

The evolution characteristics of the distribution of elastic energy of the surrounding rock during the mining process of the 1802 working face are shown in Fig. 19. From the plan view of the distribution of elastic energy, it can be known that as the length of the working face mining increases, the range of concentrated elastic energy of the surrounding rock at the goaf boundary of 1802 also gradually increases. When the length of the working face mining increases to a certain extent, the concentration degree and range of elastic energy of the surrounding rock at the goaf boundary of 1802 tend to be stable. From the section view of the distribution of elastic energy, it can be known that the elastic energy in the model is mainly distributed in Coal 8 and the top and bottom floor rock layers nearby, and the peak value of concentrated elastic energy is distributed within the range of both ends of the goaf in 1802. With the increase of the length of the working face mining, there is no obvious change in the distribution characteristics of the surrounding rock elastic energy.

(3) The evolution law of the distribution of the plastic zone

The extraction of the distribution of the plastic zone of the surrounding rock during the excavation process of the 1802 working face is shown in Fig. 20. From the plan e distribution map of the plastic zone, it can be known that as the working face continues to be excavated, the range of the plastic zone on both sides of the 1802 goaf gradually increases and tends to be stable, and the lateral plastic zone range of the goaf is about 5–20 m. From the sectional view of the distribution of the plastic zone, it can be known that the range of the plastic zone of the surrounding rock above and below the 1802 goaf does not show the rule of increasing or decreasing with the excavation of the working face. When the working face increases from excavating 600 m to excavating 1000 m, and from excavating 1800 m to excavating 2600 m, the development height of the plastic zone above the 1802 goaf increases significantly, increasing from 36 to 54 m, and from 21 to 90 m respectively. However, when it increases from excavating 2600 m to excavating 3400 and 3900 m, the range of the plastic zone above the goaf is somewhat reduced. Combined with the stratum distribution of the coal seam and its top and bottom floor and the research results of the width of the working face, it can be known that the range of the plastic zone is mainly concentrated and distributed in the complex stratum group composed of the rock layer with a single layer thickness less than 10 m above and below the coal seam. The thicker the stratum group, the larger the plastic zone, and the thinner the stratum group, the smaller the plastic zone.

The characteristic of the abutment stress distribution zone in the mining process of the first mining face

In conjunction with the geological conditions, a further analysis is conducted on the distribution and evolutionary characteristics of the stress field and energy field of the surrounding rock during the mining of the 1802 face. Extract the distribution curves of the advanced abutment stress and elastic strain energy in the middle of the 1802 working face ($Y = 2265$) when the mining length in the numerical study is sequentially 100, 150, 200, 250, 300, 600, 1000, 1400, 1800, 2200, 2600, 3000, 3600, 3850, 3900, 3950, 4000, 4050, 4100 m (from the initial mining to the end of the working face mining), as shown in Fig. 21, the statistics of the peak stress value and its advanced distance in each mining stage are as shown in Table 3.

Analyzing Fig. 21 and Table 3, it can be known that in the early stage of mining in the 1802 working face, as the width of the working face mining increases, the disturbance of the working face mining on the overlying rock formation becomes increasingly larger, the activity of the roof rock formation is more intense, and the advanced bearing stress of the surrounding rock shows an overall increasing rule. After the 1802 working face is mined to “become square”, the distribution of the peak bearing stress of the working face is relatively stable, and the influence of the increase in the mining length on the peak value of the advanced bearing stress gradually decreases. Statistical analysis shows that the peak values of the advanced bearing stress and the elastic strain energy are mainly distributed at the position of 10–20 m in advance of the working face. The advanced position of the peak bearing stress increases gradually from 10 to 20 m as the width of the working face mining increases. By comparing the size of the stress peak of the coal seam and the size of the original rock stress, the size of the peak bearing stress in advance is between 31 and 40 MPa, and the concentration degree is about 1.45–1.7. It should be noted that in this numerical study, the size of the numerical simulation model is large, and the overall size of the model grid is large. Therefore, there will be a certain deviation between the calculated results of the bearing stress advanced influence range and the actual situation on site. By analyzing the curvature change of the advanced bearing stress curve, the advanced bearing stress influence range is approximately 150–200 m.

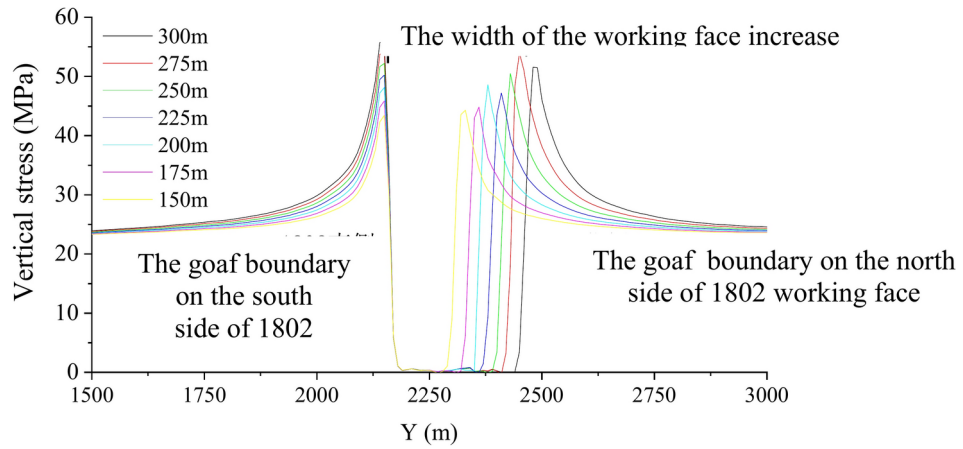


Fig. 12. The vertical stress distribution curve of the surrounding rock along the coal seam at the section where $X = 3230$ m.

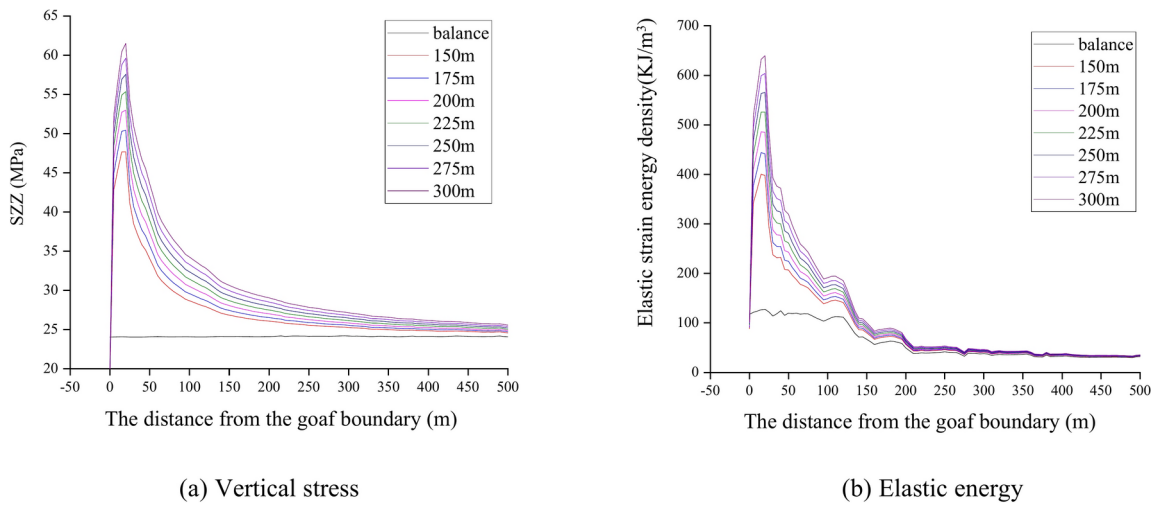


Fig. 13. The stress and elastic energy distribution of surrounding rock at the goaf boundary on the south side of the 1802 working face ($Y = 2165$ m).

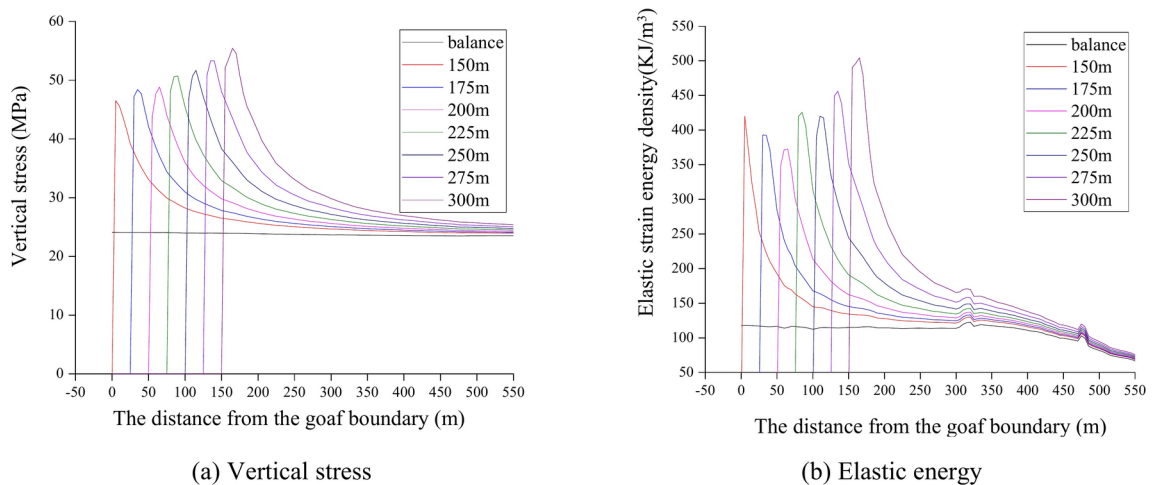


Fig. 14. The distribution of surrounding rock stress and elastic energy at the goaf boundary on the south side of the 1802 working face ($Y = 2315$ 2465 m).

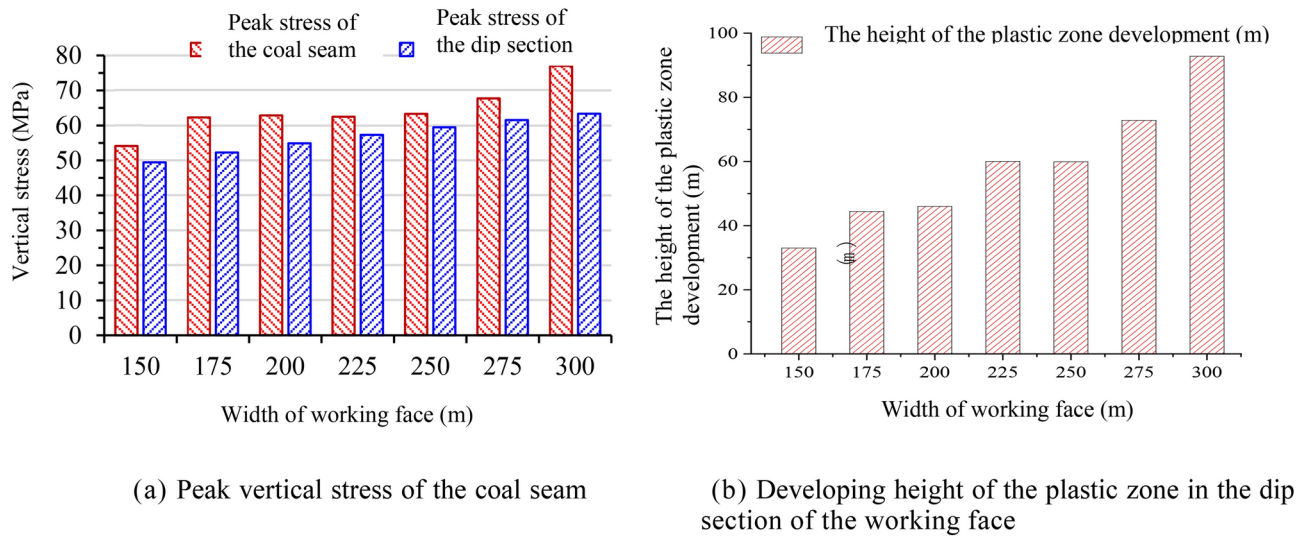


Fig. 15. The variation of surrounding rock stress and plastic zone height with the working face width.

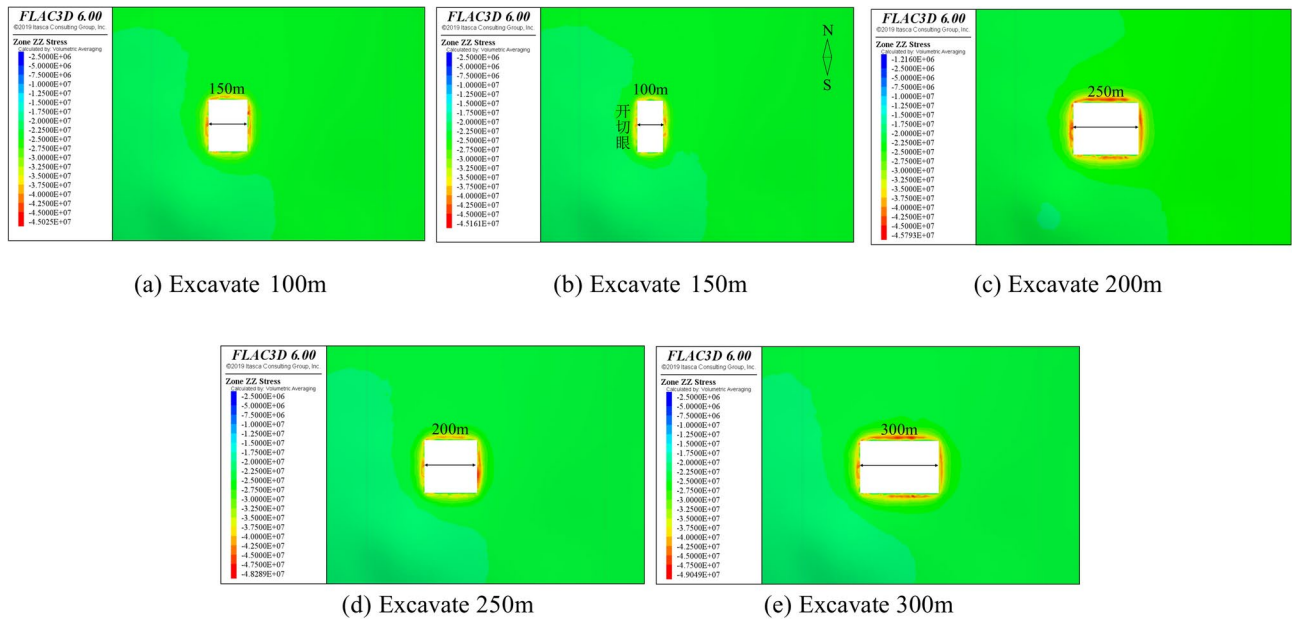
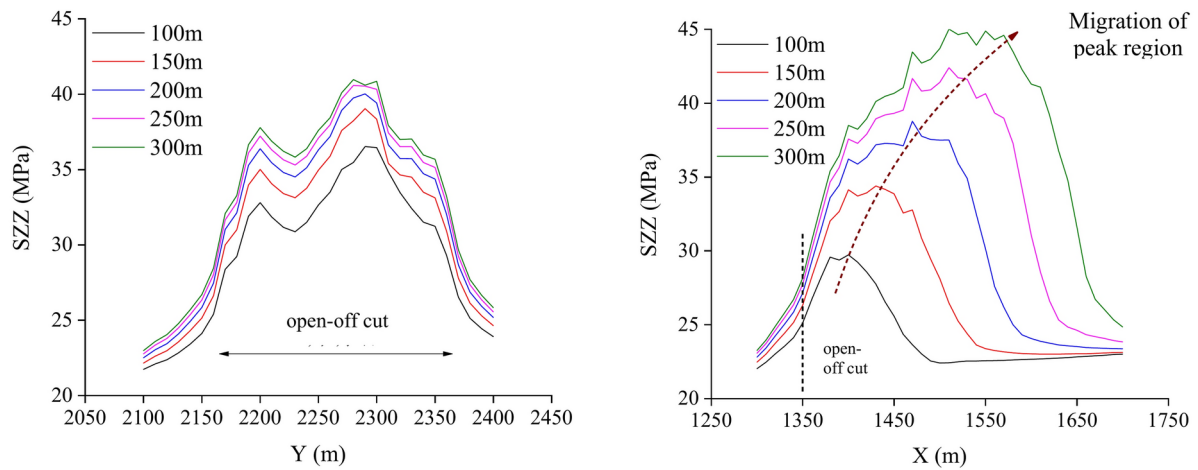


Fig. 16. Stress distribution nephogram of the surrounding rock of the goaf boundary before and after the “squaring” of the 1802 working face.

Conclusion and prospect

The geological condition of the first pan area of Xinzhuang Coal mine is complicated, which is affected by many factors such as syncline structure, buried depth of coal seam, thickness of surface soil layer, thickness of coal seam, inclination of coal seam and hard roof. In this study, the west wing of Coal 8 Pan area was selected as a typical representative, and a large-scale 3D fine numerical model was established including the above complex factors, in order to obtain the characteristics of the surrounding rock supporting stress distribution zone during



(a) Stress distribution of the goaf boundary on the side of the open-off cut (b) Stress distribution of the goaf boundary on the south side

Fig. 17. Evolution of the stress distribution of the surrounding rock of the goaf boundary before and after the “squaring” of the 1802 working face (along the coal seam).

the mining process of the working face under complex conditions through numerical simulation, and provide support for regional anti-scour design. The main conclusions are as follows:

- (1) The study reveals the distribution characteristics of mining stress, elastic energy accumulation and plastic zone distribution at different widths of the first mining face, and determines the reasonable width of the working face

The stress concentration degree and range, elastic energy concentration degree and range, plastic zone range of coal seam increase with the increase of the width of the first mining face. When the width of the first mining face increases from 150 to 300 m, the peak stress of the coal seam increases from 54.15 to 76.99 MPa, the elastic energy increases from 400 to 640 kJ/m³, the development height of the plastic zone increases from 34 to 93 m, and these parameters increase significantly when the width of the working face is greater than 250 m. According to the requirement of impact risk assessment index on the width of the working face, it is considered that the width of the working face should be greater than 175 m but less than 250 m, and the designed working face width of 200 m in Xinzhuang Coal mine is more reasonable.

- (2) The evolutionary laws of mining stress, elastic energy accumulation and plastic zone distribution and their influencing factors are revealed in the study

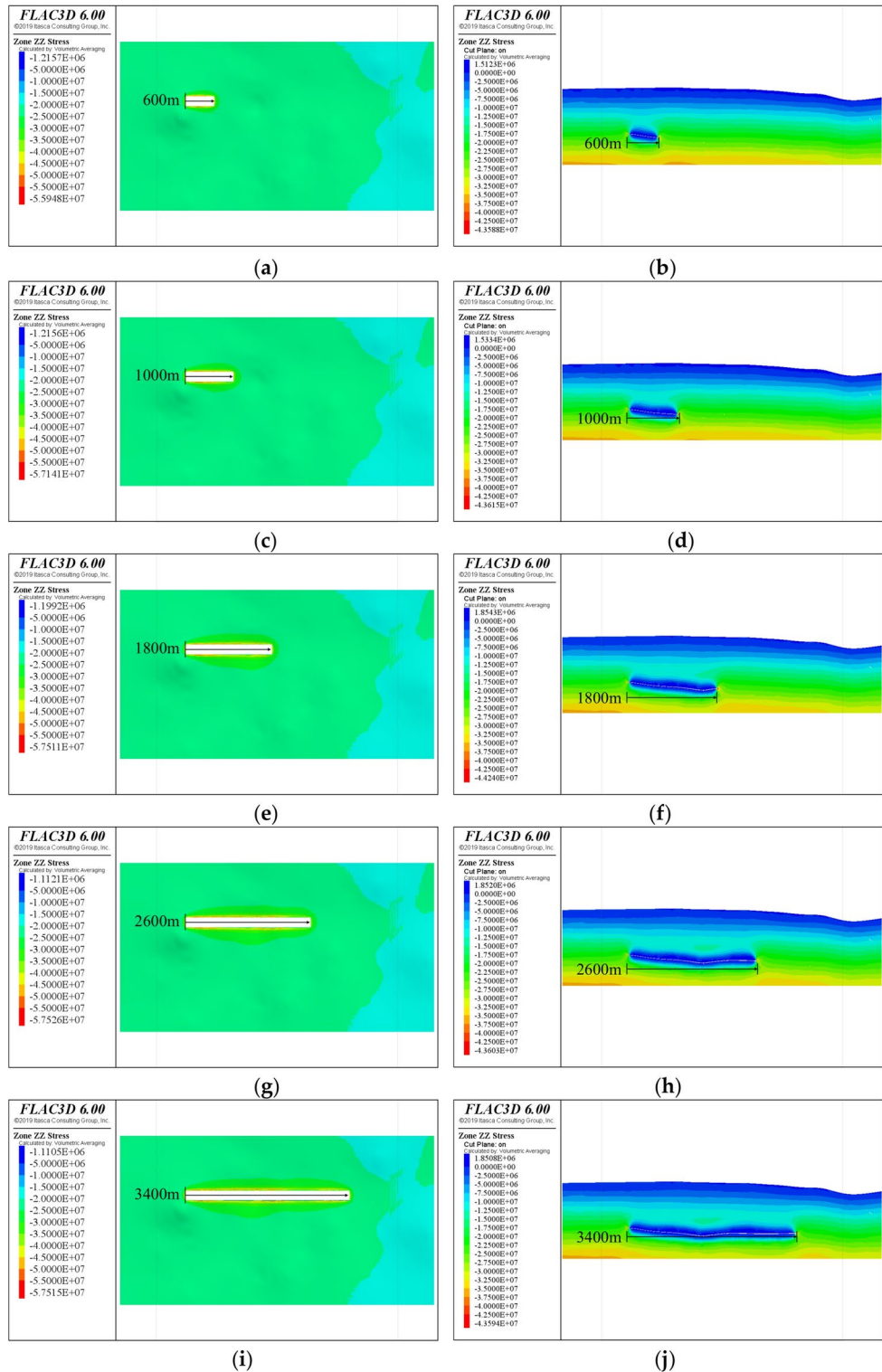


Fig. 18. The stress distribution of surrounding rock during the mining process of the 1802 working face (the profile is taken from the middle of the working face, where $Y = 2265$ m): (a) Plane stress distribution after 600 m excavation; (b) Profile stress distribution after 600 m excavation; (c) Plane stress distribution after 1000 m excavation; (d) Profile stress distribution after 1000 m excavation; (e) Plane stress distribution after 1800 m excavation; (f) Profile stress distribution after 1800 m excavation; (g) Plane stress distribution after 2600 m excavation; (h) Profile stress distribution after 2600 m excavation; (i) Plane stress distribution after 3400 m excavation; (j) Profile stress distribution after 3400 m excavation; (k) Plane stress distribution after 3900 m excavation; (l) Profile stress distribution after 3900 m excavation.

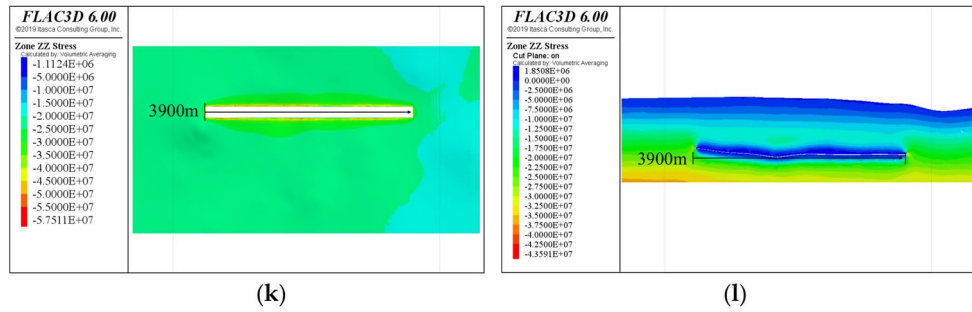


Figure 18. (continued)

The results show that the leading bearing stress is greater than the lateral bearing stress before the working face is squared, while the leading bearing stress is smaller than the lateral bearing stress after the working face is squared. During the mining process of the first mining face, there are three high mining dynamic concentration areas near the cut hole, near the strike middle syncline axis and in the second half of the working face, which are not completely consistent with the location of the stress area of the high plain rock, mainly affected by the layer spacing between the hard overlying roof and the coal seam. The smaller the layer spacing, the higher the mining stress, and the two are negatively correlated. In general, the concentration degree of mining-induced stress at the head mining face is 1.45–1.7, the peak stress is located at the depth of the coal body 10–20 m, the influence range of mining-induced stress is 150–200 m, the concentration degree of elastic energy is 1.7–2.5, and the concentration area of elastic energy is the coal body and its adjacent top and floor strata within 20–200 m of the goaf boundary. The peak elastic energy is located in the depth of coal body about 20 m, the plastic zone range is 5–20 m, the development height of plastic zone is about 20–90 m, and the development depth of plastic zone under the coal seam is about 8–30 m.

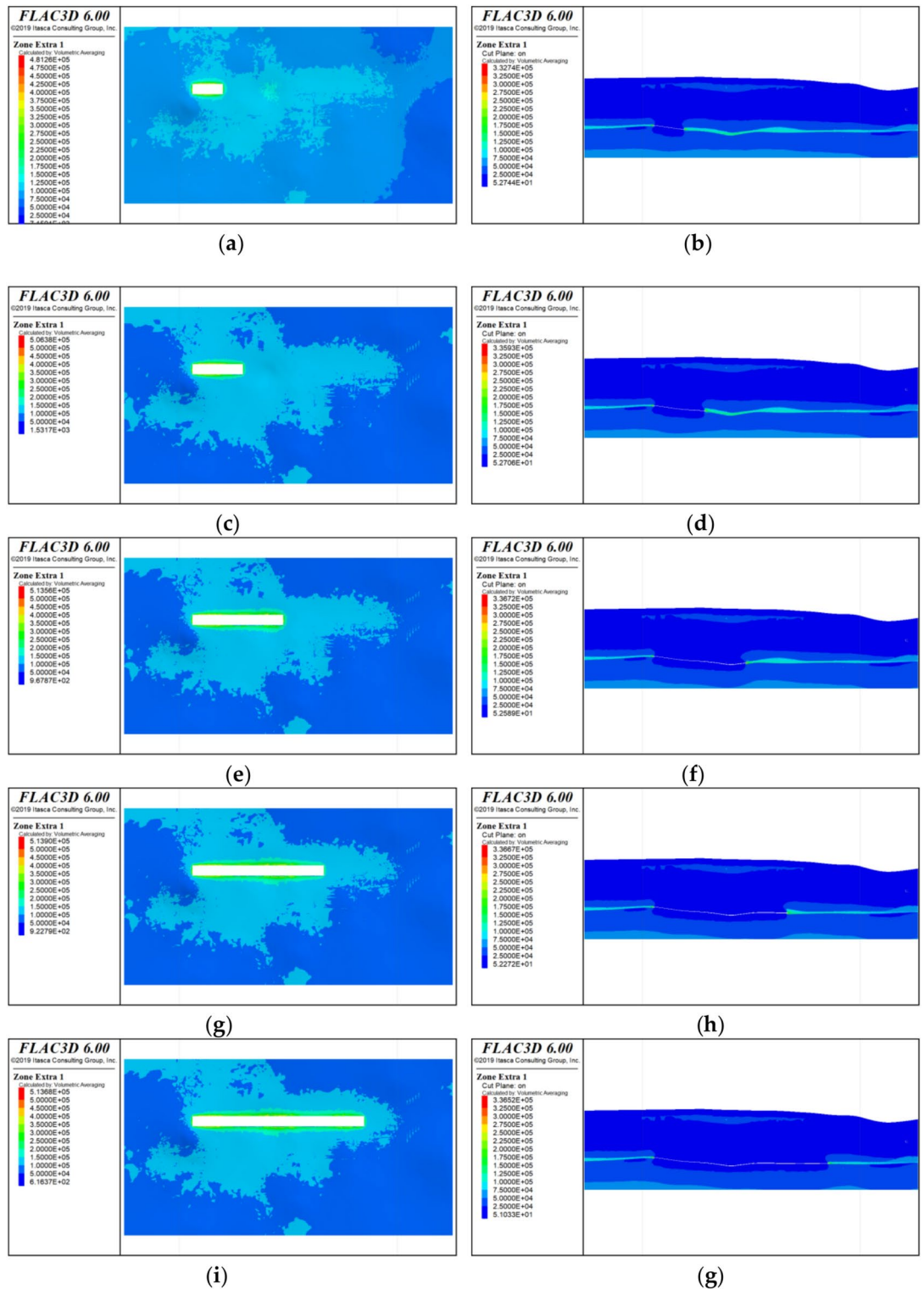


Fig. 19. The elastic energy distribution of the surrounding rock during the mining process of the 1802 working face: (a) Plane elastic energy distribution after 600 m excavation; (b) Profile elastic energy distribution after 600 m excavation; (c) Plane elastic energy distribution after 1000 m excavation; (d) Profile elastic energy distribution after 1000 m excavation; (e) Plane elastic energy distribution after 1800 m excavation; (f) Profile elastic energy distribution after 1800 m excavation; (g) Plane elastic energy distribution after 2600 m excavation; (h) Profile elastic energy distribution after 2600 m excavation; (i) Plane elastic energy distribution after 3400 m excavation; (j) Profile elastic energy distribution after 3400 m excavation; (k) Plane elastic energy distribution after 3900 m excavation; (l) Profile elastic energy distribution after 3900 m excavation.

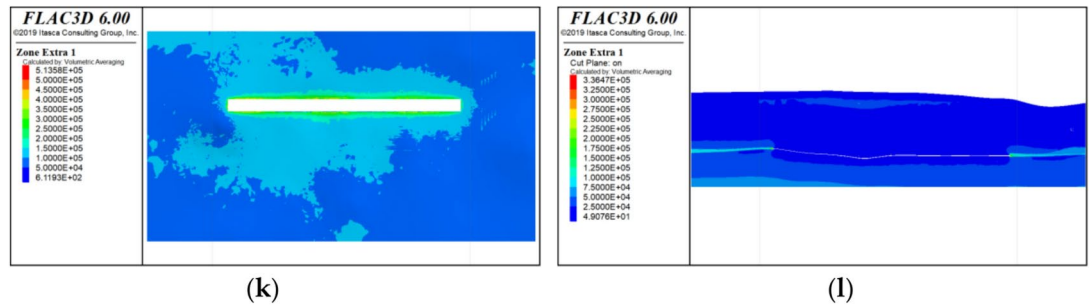


Figure 19. (continued)

In the future, the research in this field can be carried out from the following directions. In terms of theoretical research, the mining stress mechanics model of surrounding rock under multi-factor coupling is further improved, and the nonlinear mechanical behavior of rock, the influence of geological structure and the interaction between different rock layers are considered, so as to improve the accuracy and applicability of the theoretical model. In terms of numerical simulation, more advanced numerical simulation software and algorithms are developed to improve the simulation accuracy of complex geological physical behavior, and fully consider the characteristics of rock mass heterogeneity, anisotropy and rheology, so that the simulation results are closer to the actual situation.



Fig. 20. The distribution of the plastic zone of the surrounding rock during the mining process of the 1802 working face: (a) Plane plastic zone distribution after 600 m excavation; (b) Profile plastic zone distribution after 600 m excavation; (c) Plane plastic zone distribution after 1000 m excavation; (d) Profile plastic zone distribution after 1000 m excavation; (e) Plane plastic zone distribution after 1800 m excavation; (f) Profile plastic zone distribution after 1800 m excavation; (g) Plane plastic zone distribution after 2600 m excavation; (h) Profile plastic zone distribution after 2600 m excavation; (i) Plane plastic zone distribution after 3400 m excavation; (j) Profile plastic zone distribution after 3400 m excavation; (k) Plane plastic zone distribution after 3900 m excavation; (l) Profile plastic zone distribution after 3900 m excavation.

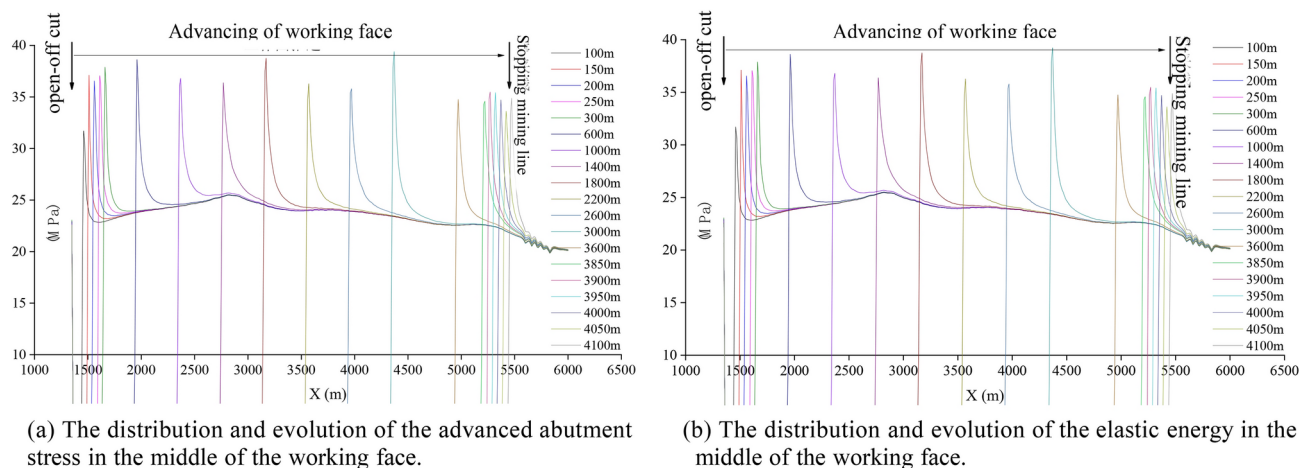


Fig. 21. The evolution characteristics of advanced stress and energy distribution during the mining process of the 1802 working face.

Mining length (m)	Stress peak (Mpa)	Advanced distance of stress peak	Elastic energy peak value (KJ/m ³)	The advanced distance of the elastic energy peak value (m)
100	31.71	10	189.28	10
150	37.11	10	242.00	10
200	36.56	10	246.04	10
250	37.06	10	248.96	10
300	37.88	10	269.36	10
600	38.62	10	269.36	10
1000	36.80	20	240.44	10
1400	36.38	20	234.96	20
1800	38.75	20	252.51	10
2200	36.28	20	217.06	10
2600	35.79	20	223.55	10
3000	39.40	20	253.05	10
3600	34.75	20	200.21	20
3850	34.58	20	210.89	10
3900	35.48	20	214.72	10
3950	35.42	20	202.11	20
4000	34.70	20	197.47	20
4050	33.62	20	192.03	20
4100	34.88	20	201.04	20

Table 3. Statistics of the peak value of advanced bearing stress and elastic energy during the mining process of the 1802 working face.

Data availability

The datasets used and/or analysed during the current study available from the corresponding author on reasonable request.

Received: 19 September 2024; Accepted: 28 April 2025

Published online: 14 May 2025

References

- He, S. Q. et al. Multi-parameter integrated early warning model and an intelligent identification cloud platform of rockburst. *J. China Univ. Min. Technol.* **51**, 850–862 (2022).
- Xie, H. P. et al. Theoretical and technological conception of the fluidization mining for deep coal resources. *J. China Coal Soc.* **42**, 547–556 (2017).
- Qi, Q. X. et al. Theory and technical framework of prevention and control with different sources in multi-scales for coal and rock dynamic disasters in deep mining of coal mines. *J. China Coal Soc.* **7**, 1801–1810 (2018).
- Dou L. M., He X. Q. *Impact Ore Pressure Prevention Theory and Technology* (China Univ. Min. Univ., 2001).
- Qi, Q. X., Dou, L. M. *Intellectual Pressure Theory and technology* (China Univ. Min. Univ., 2008).

6. Cao, A. Y. et al. Dynamic manifestation mechanism of mining on the island coalface along fault and dynamic pre-warning of seismic waves with seismic tomography. *J. Min. Saf. Eng.* **34**, 411–417 (2017).
7. Pan, J. F. et al. The top board “artificial liberation layer” to prevent the impact ground pressure method, mechanism and application. *J. China Coal Soc.* **48**, 636–648 (2023).
8. Wang, H. W. et al. Abrupt effect of coupling instability of fault overburden induced by mining. *J. Coal Sci.* **48**, 2961–2975 (2023).
9. He, X. Q. et al. Typical nearly upright coal seam group impact ground pressing mechanism, monitoring and early warning research. *Tunn. Undergr. Space Technol.* **49**, 13–22 (2021).
10. Pan, J. F. et al. Pressing the theory and technology of the static loading of static loads in the deep lanes. *J. China Coal Soc.* **45**, 1607–1613 (2020).
11. Tan, Y. L. et al. Deep coal lane gangs to seduce the mechanism and “unload-solid” collaborative control research. *J. China Coal Soc.* **45**, 66–81 (2020).
12. Yang, R. S. et al. Model experiment on dynamic behavior of jointed rock mass under blasting at high-stress conditions. *Tunn. Undergr. Space Technol.* **74**, 145–152 (2018).
13. Yang, L. Y. & Ding, C. X. Fracture mechanism due to blast-imposed loading under high static stress conditions. *Int. J. Rock Mech. Min. Sci.* **107**, 150–158 (2018).
14. Zhu, Q. J. et al. The design of the evaluation system of the coal mine impacting system and its implementation. *J. North China Univ. Sci. Technol.* **19**, 1–7 (2022).
15. Wang, C. W. et al. Analysis on control action of geologic structure on rock burst and typical cases. *J. China Coal Soc.* **37**, 263–268 (2012).
16. Wang, H. B. et al. Wudong coal mine urgent sanded coal sea anti-bringing technology. *Autom. Operating* **48**, 58–61 (2022).
17. Xu, W. Research on monitoring technology and application of surrounding rock stress in mining space. China University of Mining and Technology (2012).
18. Si, X. Rock Burst simulation test and mechanism study of deep high stress hard rock tunnel surrounding rock. Central South University (2022).

Author contributions

Conceptualization, X.M.; methodology, E.W.; software, X.M. and E.W.; validation, W.W. and B.W.; formal analysis, X.M. and E.W.; investigation, X.M. and Q.G.; resources, Z.L.; data curation, Q.G.; writing—original draft preparation, X.M. and E.W.; writing—review and editing, X.M. and E.W.; visualization, Y.L.; supervision, B.H. and F.S.; project administration, X.M. and B.H.; funding acquisition, E.Y. and X.M. All authors have read and agreed to the published version of the manuscript.

Funding

This research was funded by the National Natural Science Foundation of China (Grant No. 52064042), the China Postdoctoral Science Foundation (Grant No. 2023MD734191), the Program for Young Talents of Science and Technology in Universities of Inner Mongolia Autonomous Region (Grant No. NJYT24040), the Fundamental Research Funds for Inner Mongolia University of Science & Technology (Grant No. 2023QNJS112), the Innovation Fund Project of Inner Mongolia University of Science & Technology (Grant No. 2019QDL-B34), the Open Fund Project of the State Key Laboratory of Deep Geotechnical Mechanics and Underground Engineering of China University of Mining and Technology (Beijing) (SKLGDUEK2020), the Huaneng Group Headquarters Science and Technology Project (HNKJ20-H32, HNKJ21-H56-10).

Declarations

Competing interests

The authors declare no competing interests.

Additional information

Correspondence and requests for materials should be addressed to E.W.

Reprints and permissions information is available at www.nature.com/reprints.

Publisher’s note Springer Nature remains neutral with regard to jurisdictional claims in published maps and institutional affiliations.

Open Access This article is licensed under a Creative Commons Attribution-NonCommercial-NoDerivatives 4.0 International License, which permits any non-commercial use, sharing, distribution and reproduction in any medium or format, as long as you give appropriate credit to the original author(s) and the source, provide a link to the Creative Commons licence, and indicate if you modified the licensed material. You do not have permission under this licence to share adapted material derived from this article or parts of it. The images or other third party material in this article are included in the article’s Creative Commons licence, unless indicated otherwise in a credit line to the material. If material is not included in the article’s Creative Commons licence and your intended use is not permitted by statutory regulation or exceeds the permitted use, you will need to obtain permission directly from the copyright holder. To view a copy of this licence, visit <http://creativecommons.org/licenses/by-nc-nd/4.0/>.

© The Author(s) 2025